A)

B)

Table S1. Comparisons of best fitting (first-order, non-linear, density-linked stochastic) models for first- or fourth-order data, and parameter estimates derived from model averaging.
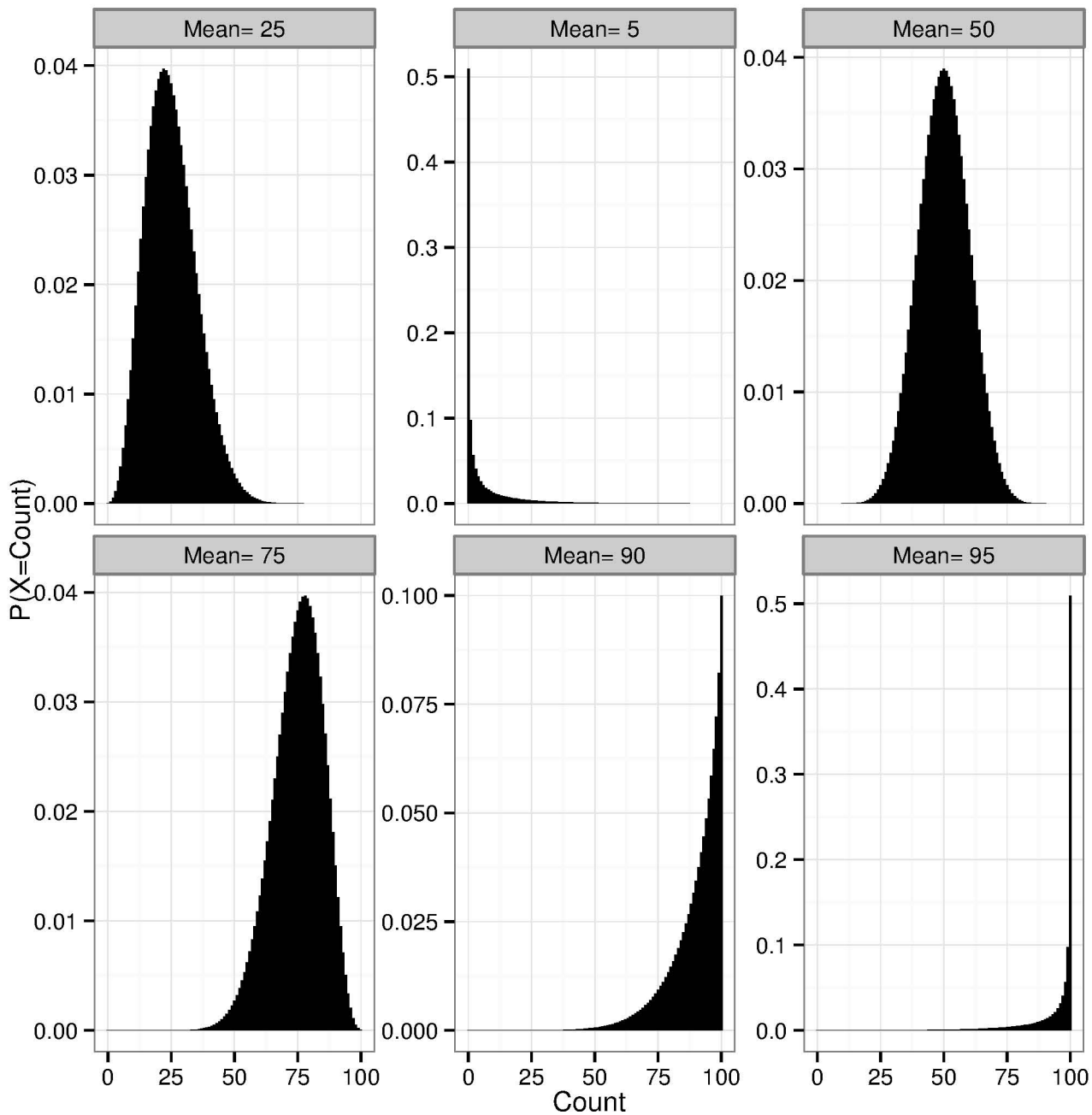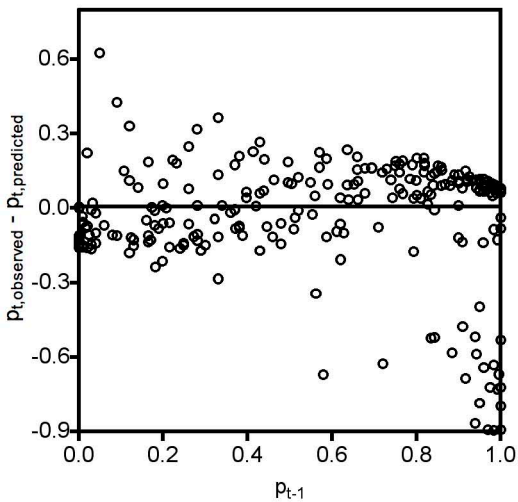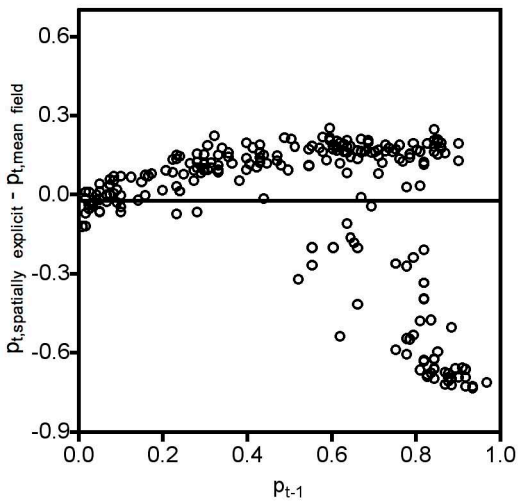
	4 year lag data			1 year lag data		
		Model Averaged			Model Averaged	
	Best Fit	Mean	CI	Best Fit	Mean	CI
I	0.053	0.052	0.047, 0.057	0.071	0.069	0.063, 0.076
r	0.522	0.530	0.508, 0.552	0.600	0.599	0.592, 0.605
α_1	-0.524	-0.533	-0.558, -0.508	-0.615	-0.611	-0.625, -0.597
β	0*	0.002	-0.0005, 0.004	0.014	0.011	0.006, 0.015
c	0*	44.84	-69.42, 159.10	28.62	22.14	10.52, 33.77
α_2	0*	-2×10^{-5}	$-7 \times 10^{-5}, 2 \times 10^{-5}$	0*	0*	0*
β_2	0*	0.001	-0.001, 0.003	0*	0*	0*
c_2	1*	1.011	0.968, 1.053	1*	1*	1*
α_3	0*	-1×10^{-5}	$-4 \times 10^{-5}, 1 \times 10^{-5}$	0*	0*	0*
β_3	0*	0.002	-0.002, 0.006	0*	0*	0*
c_3	1*	0.998	0.990, 1.006	1*	1*	1*
α_4	0*	1×10^{-5}	$-1 \times 10^{-5}, 4 \times 10^{-5}$	0*	0*	0*
β_4	0*	4×10^{-7}	$-9 \times 10^{-7}, 2 \times 10^{-6}$	0*	0*	0*
c_4	1*	1.004	0.987, 1.022	1*	1*	1*
x	-2.959	-2.962	-3.165, -2.760	-2.570	-2.596	-2.756, -2.435
y	-2.023	-1.991	-2.200, -1.781	-2.308	-2.288	-2.516, -2.060
z	13.13	13.32	11.957, 14.683	8.983	8.859	7.992, 9.726
μ_d	0.393	0.393	0.372, 0.415	0.392	0.391	0.370, 0.413
σ^2_d	0.090	0.090	0.088, 0.092	0.090	0.090	0.088, 0.092
j	-3.143	-3.133	-3.434, -2.832	-3.172	-3.115	-3.473, -2.756

| k | 2.225 | 2.213 | 2.000, 2.427 | 2.288 | 2.232 | 1.930, 2.533 |

*parameter fixed a priori.

Supporting Text S1.

The Beta-Binomial Distribution

Beta-binomial distributions provide a flexible framework for modeling bounded discrete

distributions (Crowder 1978, Kendall 1998). When bounded by the interval [0,1], the beta-

binomial can be thought of as a description of a distribution of events where the outcome of an

individual event has two possibilities (present/absent, alive/dead, etc.), the binomial portion of

the distribution, but that the probability of the event occurring varies, for example as the

environment fluctuates, which is described by the beta portion of the distribution (Richards

2008). The benefit of using the beta-binomial over a continuous beta distribution in situations

such as ours is that observations of 0 and 1 are permitted. The equations and discussion that

follow are only strictly applicable to a distribution bounded by [0,1].

The beta-binomial distribution is controlled by two positive-valued shape parameters (a, b),

which define the beta distribution component, and the sample size (N), which defines the

subsequent binomial component of the distribution. Depending on the shape parameters, the

resulting distribution can be approximately uniform ($a = b = 1$), symmetrically unimodal ($a = b >$

1), bimodal (a, $b < 1$) or skewed ($a \neq b$) (e.g. Fig. S2). For convenience and efficiency of model

fitting, it is sometimes useful to work with the sum of the shape parameters ($\phi = a + b$) (Morris

1997).

The shape parameters of the beta portion of the distribution are related to the mean (μ) and

variance (σ^2) of the distribution. Hence, when σ^2 is fixed the shape of the distribution varies

from strongly skewed right to unimodal to strongly skewed left as μ increases from its minimum

to maximum value (0-1 in our analyses; Fig. S3).

The mean and variance of the beta portion of the distribution are related to the shape parameters through the following relationships:

$$\mu = \frac{a}{\phi}$$

$$\sigma^2 = \frac{\mu \cdot (1 - \mu)}{\phi + 1}$$

Equations S1

or, after rearranging:

$$a = \phi \cdot \mu$$

$$b = \phi \cdot (1 - \mu)$$

Equations S2.

Hence, we can define the beta-binomial distribution given an expected value (e.g., a function describing predicted mean population size) and rules for the behavior of the variance of that function. We apply these relationships in our model fitting procedure by defining a population dynamic function to fit and rules for how variance behaves across that function, following either traditional assumptions (σ^2 is a constant) or assumptions that variation depends on density.

Under constant σ^2, the shape parameters vary with the mean such that:

$$\phi = (\mu - \mu^2 - \sigma^2)/\sigma^2 \qquad (0 < \mu < 1) \qquad \text{Equation S3.}$$

Note that this equation accounts for constant process error (beta function portion of the distribution), not the sampling error (binomial portion), which changes the overall distribution such that variance is slightly higher at intermediate (≈ 0.5) values of μ compared to values near the ends of the distribution (0 or 1).

When a and b are constants, σ^2 naturally varies with mean predicted abundance, such that variance approaches 0 when μ approaches 0 or 1. This pattern qualitatively does not describe our data, and model fitting using this special case of varying σ^2 consequently provides very poor fits. For this reason, we do not discuss this situation further.

For more flexible density-linked variance patterns, we used the relationship:

$$\phi = 1 + \exp(-(x + y \cdot p_{t-1}^{z}))$$
$\qquad$ Equation S4.

Focusing on ϕ in this equation, rather than σ^2 directly, still allows variance to increase or decrease with abundance (p_{t-1}), but also provides a smooth function that increases the efficiency of fitting algorithms, and that helps maintain constraints that the shape parameters be positive and that the variance distribution be unimodal and positive during the fitting procedure. The negative sign in the exponential term is included so that increasing any of variance control parameters (x, y, z) results in increasing variance, thereby making interpretation of parameters easier.

The parameters that maximize the fit of a model given a set of data should be those that maximize the probability mass function (PMF) for the beta-binomial, or alternatively minimize, the $-\log$(PMF). For our 16 quadrats with t_{max} time intervals (15-17), the latter is given by the equation:

$$-\log(PMF) = -\sum_{q=1}^{16} \sum_{t=1}^{t_{max,q}} \log\left(\binom{N_q}{\Omega_{q,t}} \cdot \left(\frac{Beta(\Omega_{q,t} + a_{q,t}, N_q - \Omega_{q,t} + b_{q,t})}{Beta(a_{q,t}, b_{q,t})}\right)\right)$$
$\qquad$ Equation S4,

where $\Omega_{q,t}$ is the observed abundance in quadrat q at time t, N is the sample size in quadrat q, *Beta* is the beta function with shape parameters a, and b. Note that because a and b depend on the expected function and variance, which change with differing density in each quadrat at each sample point, these values vary for each different sample point in each different quadrat.

The combinatorial term in Equation S4 creates computational accuracy problems due to very large factorial numbers at high N. Therefore in our calculations, we used a form with a large number approximation to estimate the PMF:

$$-\log(PMF) = -\sum\sum \log\left(\frac{Beta(\Omega_{q,t} + a_{q,t}, N_q - \Omega_{q,t} + b_{q,t})}{(N_q + 1) \cdot Beta(\Omega_{q,t} + 1, N_q - \Omega_{q,t} + 1) \cdot Beta(a_{q,t}, b_{q,t})}\right)$$

Equation S5.

Beta-Binomial References

Crowder MJ (1978) Beta-binomial ANOVA for proportions. Appl Stat-J Roy St C 27: 34-37.

Kendall B (1998) Estimating the magnitude of environmental stochasticity in survivorship data.
Ecol Appl 8: 184-193.

Morris WF (1997). Disentangling effects of induced plant defenses and food quantity on
herbivores by fitting nonlinear models. Am Nat 150: 299–327.

Richards S (2008) Dealing with overdispersed count data in applied ecology. J Appl Ecol 45:
218-227.

Supporting Text 2

Effect of Localized Disturbance Interactions

Prior studies (Robles et al. 1995, Wootton 2001b) suggest one mechanism that might contribute to DLS in mussel beds: the transmission of wave disturbance among adjacent individuals when neighbors attach their byssal threads to each other rather than to the rock substrate. Wootton (2001b) developed, parameterized and analyzed a cellular automata model of this mussel bed system to explore the role of spatially localized interactions within the community. This model, which simulated the community dynamics within 6 x 6 cm cells of an intertidal bench ~6 x 18 m, effectively recaptured spatial patterning of the system when wave disturbance was propagated by local interactions among mussels via mutual byssal thread attachment. If spatially localized interactions underlie key aspects of the observed DLS, then when spatial points in the simulation are aggregated into population data at the scale of the quadrats used in this study, DLS should emerge.

To convert the cellular automata to a population model we randomly placed 16 10 x 10 cell quadrats on the 100 x 300 grid used in the model to scale the system to a typical rock bench at this site. We then ran the cellular automata for 500 simulated years to eliminate transient patterns and subsequently collected data on predicted mussel cover in each quadrat for a period of 17 simulated years. To isolate the effects of local interactions on population dynamics, we compared these dynamics to a mean-field model lacking spatially local interactions (i.e., a spatial version of a Markov chain model parameterized for the system using the same initial conditions; Wootton 2001a, 2004, 2013).

Essential features of observed DLS emerged when spatially-localized interactions act in concert with stochastic disturbance events (Fig. S4). This pattern indicates that spatially-local

interactions are the cause of the pattern in the simulations and can contribute key aspects of the observed dynamics.

Supporting Text 2 References

Robles C, Sherwood-Stephens R, Alvarado M (1995) Responses of a key intertidal predator to varying recruitment of its prey. Ecology 76: 565-579.

Wootton JT (2001a) Local interactions predict large-scale pattern in an empirically-derived cellular automata. Nature 413: 841-843.

Wootton JT (2001b) Prediction in complex communities: analysis of empirically-derived Markov models. Ecology 82: 580-598.

Wootton JT (2004) Markov chain models predict the consequences of experimental extinctions. Ecol Lett 7: 653-660.

Wootton JT (2013) An experimental test of multi-species Markov models: Are barnacles long-term facilitators of mussel bed recovery? Bull Mar Sci 89: 337-346.